Improved variational wave functions for SU(3) Hamiltonian lattice gauge theory

Chris Long and D. Robson
Department of Physics, Florida State University, Tallahassee, Florida 32306

Siu A. Chin
Center for Theoretical Physics, Department of Physics, Texas A&M University, College Station, Texas 77840

(Received 3 November 1987)

We study improved variational wave functions for SU(3) Hamiltonian lattice gauge theory by comparing variational ground-state energies and scalar-glueball masses. Variational wave functions that include twisted six-link Wilson loops and plaquettes are significantly better than those that include only plaquettes for calculating the ground-state energy and the scalar-glueball mass. The calculated glueball mass approaches scaling, suggesting that further improvements can be made by including more loops.

I. INTRODUCTION

The Hamiltonian lattice gauge theory provides a direct way of calculating the low-lying spectrum of the gauge field sector of QCD (Ref. 1). Monte Carlo calculations in the Hamiltonian form of the theory appear to be less computationally intensive than those in the Lagrangian form because they use a three-dimensional spatial lattice rather than a four-dimensional spacetime lattice. The Hamiltonian form has the advantage that energy observables such as glueball masses and the string tension appear as eigenvalues.

Exact ground-state expectation values of the lattice Hamiltonian can be calculated by Monte Carlo methods,[2] but much less computer resources are needed if a sufficiently accurate variational wave function can be found. It is therefore important to find accurate variational wave functions that are not too difficult to calculate.

We consider the Kogut-Susskind lattice Hamiltonian[3]

$$H=\frac{g^2}{a}\left[\frac{1}{2}\sum_{l,a}E_l^aE_l^a+\frac{2N}{g^4}\sum_p(1-\mathrm{Re\,Tr}U_p)\right], \quad (1)$$

where a, l, and p are color, link, and plaquette labels and

$$[E_l^a,U_{l'}]=\delta_{ll'}T^aU_l\ . \quad (2)$$

Here T^a are the generators of SU(N) normalized so that

$$\mathrm{Tr}(T^aT^b)=\tfrac{1}{2}\delta_{ab}\ . \quad (3)$$

The commonly used one-parameter variational wave function

$$\phi_0=\exp\left[AN\sum_p\mathrm{Re\,Tr}U_p\right] \quad (4)$$

is sometimes called the "independent plaquette" wave function. This could be misleading because the plaquettes are not independent in three or more dimensions since the plaquettes that enclose any volume are correlated by the Bianchi relations.[4] This simple wave function is exact in the limit of strong coupling and surprisingly accurate in intermediate coupling. It leads to a variational ground-state energy that is only slightly higher than the exact energy, and it seems to improve with increasing size N of the gauge group.[5] Calculations of the scalar-glueball mass using ϕ_0 combined with the simplest excited-state wave function $F\phi_0$, where

$$F=P-\langle P\rangle \quad (5)$$

and

$$P=\frac{1}{N}\frac{1}{3L^3}\sum_p\mathrm{Re\,Tr}U_p\ , \quad (6)$$

show evidence for scaling in SU(6) and possibly SU(5) (Ref. 5). Throughout this paper angular brackets denote an expectation value with respect to the variational ground state. Unfortunately, no evidence for scaling appears when these wave functions are used in SU(3). Because of their relevance to QCD, variational wave functions accurate enough to approach mass-gap scaling in SU(3) are highly desirable.

The wave functions can be improved by including other types of Wilson loops and adjusting their contributions with additional variational parameters. Since the one-parameter wave function ϕ_0 has the same form as the first-order term in the strong-coupling expansion,[6] it is natural to try to improve it by including loops that appear in the second term. By far the easiest to include are those that involve only functions of the trace of a single plaquette matrix. We have considered a second-order wave function of the form

$$\phi=\exp\left[\sum W_1\mathrm{Re\,Tr}U_p+W_2\mathrm{Re}(\mathrm{Tr}U_p)^2+W_3\mathrm{Tr}U_p\mathrm{Tr}U_p^\dagger\right]. \quad (7)$$

Like the one-parameter wave function, this wave function is separable in plaquette space so that the ground-state energy density is easily calculated without recourse to

Monte Carlo methods. This is done by transforming to plaquette space and performing a character expansion of the Jacobian of the transformation.[7] Minimizing the energy with respect to the three parameters gives a slightly improved variational wave function, with the energy lowered by only about 15% of the difference between the one-parameter value and the exact value. A similar result has been reported for the SU(2) case.[8] Thus, it appears that a significantly improved ground-state wave function will necessarily include more complicated loops.

II. THE TWISTED LOOPS

Link-space Monte Carlo calculations have been indispensable for both exact[2,9] and variational[5] lattice QCD calculations. They have the disadvantage that they are computationally expensive because of the requirement that a large number of matrix multiplications must be done. The required number of matrix multiplications depends on the product of the number of links per loop and the number of loops that contain a given link. The plaquettes are the only type of four-link loop, but there are three types of six-link loops as shown in Fig. 1. The loops whose shape is shown in Fig. 1(c) have been called "twisted plaquettes,"[10] but we call them simply the "twisted loops." They first appear in the third term of the strong-coupling expansion. In link-space Monte Carlo calculations, the twisted loops are the easiest type of six-link loop to include. This can be seen from Table I.

Here we concentrate on the twisted loops and define a two-parameter wave function as

$$\phi=\exp\left[AN\sum_{p}\mathrm{Re\,Tr}U_p+BN\sum_{t}\mathrm{Re\,Tr}U_t\right], \tag{8}$$

where U_t denotes the matrix formed by taking the ordered product of the six matrices associated with the links depicted in Fig. 1(c). The variational dimensionless ground-state energy density per gluon degree of freedom is then given by

$$\epsilon_0=\frac{\langle H\rangle a}{3L^3(N^2-1)}=\frac{1}{\xi}\left[\frac{1}{2}A\langle P\rangle+B\langle T\rangle+\frac{2N^2}{N^2-1}\xi^2(1-\langle P\rangle)\right], \tag{9}$$

$$T=\frac{1}{4L^3}\frac{1}{N}\sum\mathrm{Re\,Tr}U_t\ , \tag{10}$$

and

$$Ma\xi=\frac{-N^2L^3}{3}\frac{\left\langle\sum_{l,a}(E_l^aP)^2+2\gamma(E_l^aP)(E_l^aT)+\gamma^2(E_l^aT)^2\right\rangle}{\frac{1}{3}\frac{\partial\langle P\rangle}{\partial A}+\gamma\left[\frac{1}{3}\frac{\partial\langle T\rangle}{\partial A}+\frac{1}{4}\frac{\partial\langle P\rangle}{\partial B}\right]+\gamma^2\frac{1}{4}\frac{\partial\langle T\rangle}{\partial B}} \tag{17}$$

and minimized with respect to γ. The values of γ that minimize the mass gap are given in Table II.

III. METHOD OF CALCULATION

A one-hit Metropolis algorithm was used to generate the ensemble of configurations on a 4^3 lattice with period-

TABLE I. The number of Wilson loops in an L^3 lattice and the number that contains a given link.

Wilson loop	No. in an L^3 lattice	No. that contains a given link
Plaquette	$3\ L^3$	4
Twisted loop	$4\ L^3$	8
Planar 6	$6\ L^3$	12
Bent 6	$12\ L^3$	24

$$\xi=\frac{1}{Ng^2}\ . \tag{11}$$

Equation (9) actually gives one-third of the density per gluon degree of freedom to facilitate comparison with earlier work.

The values of A and B that minimize the ground-state energy density are given in Table II. In Fig. 2 the resulting ground-state energy densities are compared with those obtained from the one-parameter wave function and the exact values obtained from guided-random-walk Monte Carlo calculations.[9] Including the twisted loops lowers the energy by about 40% in the region of interest.

If ϕ is a good approximation to the exact ground state, then the 0^{++} glueball mass can be estimated by minimizing

$$M=E_1-E_0=\frac{\langle[F^\dagger,[H,F]]\rangle}{2\langle F^\dagger F\rangle} \tag{12}$$

with respect to F, where $F\phi$ is a variational excited-state wave function orthogonal to ϕ (Ref. 5). In order to include twisted loops in the excited-state projector, we used

$$F=P-\langle P\rangle+\gamma(T-\langle T\rangle)\ , \tag{13}$$

where γ is a variational parameter for the excited state. No approach to scaling behavior was observed with $\gamma=0$. The denominator above is written in terms of the derivatives

$$\frac{\partial\langle P\rangle}{\partial A}=6N^2L^3(\langle P^2\rangle-\langle P\rangle^2)\ , \tag{14}$$

$$\frac{\partial\langle P\rangle}{\partial B}=8N^2L^3(\langle PT\rangle-\langle P\rangle\langle T\rangle)=\frac{4}{3}\frac{\partial\langle T\rangle}{\partial A}\ , \tag{15}$$

$$\frac{\partial\langle T\rangle}{\partial B}=8N^2L^3(\langle T^2\rangle-\langle T\rangle^2)\ , \tag{16}$$

so that the mass can be rewritten as

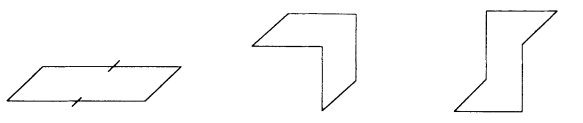

a) Planar 6 b) Bent 6 c) Twisted 6

FIG. 1. The three types of six-link Wilson loops.

TABLE II. Numerical values for the trial function parameters A,B that minimize the ground-state energy, values of the parameter γ, which minimize the scalar-glueball mass, the resulting dimensionless ground-state energy density ϵ_0, and the dimensionless scalar-glueball mass $Ma\xi$ at selected values of the coupling $\xi=1/3g^2$.

ξ	A	B	γ	ϵ_0	$Ma\xi$
0.260	0.1626	0.0072	0.3290	0.530	0.716
0.265	0.1688	0.0089	0.3890	0.538	0.698
0.270	0.1750	0.0100	0.4326	0.546	0.687
0.275	0.1806	0.0116	0.4776	0.552	0.677
0.280	0.1864	0.0130	0.5134	0.560	0.669
0.285	0.1925	0.0141	0.5423	0.567	0.662
0.290	0.1986	0.0157	0.5683	0.574	0.650
0.295	0.2051	0.0175	0.5994	0.580	0.633
0.300	0.2126	0.0192	0.6343	0.586	0.610
0.305	0.2198	0.0214	0.6735	0.593	0.586
0.310	0.2258	0.0244	0.7161	0.598	0.563
0.315	0.2311	0.0278	0.7678	0.604	0.540
0.320	0.2365	0.0307	0.8172	0.609	0.522
0.325	0.2418	0.0332	0.8470	0.614	0.511
0.330	0.2473	0.0348	0.8649	0.619	0.505
0.330	0.2523	0.0361	0.8754	0.623	0.504
0.340	0.2577	0.0375	0.9065	0.627	0.502
0.345	0.2617	0.0399	0.9600	0.632	0.498
0.350	0.2650	0.0425	1.0211	0.635	0.497

ic boundary conditions. For each point (A,B) in parameter space, 10^3 warm-up sweeps were discarded before 10^4 measuring sweeps were performed. Average values and variances of the following five quantities were measured:

$$\langle P\rangle,\ \langle T\rangle,\ \left\langle L^3\sum_{l,a}(E_l^aP)^2\right\rangle,$$
$$\left\langle L^3\sum_{l,a}(E_l^aP)(E_l^aT)\right\rangle,\ \left\langle L^3\sum_{l,a}(E_l^aT)^2\right\rangle.$$

To calculate the variance, 100 block averages of 100 sweeps each were treated as statistically independent samples.

Considerable difficulty was experienced in finding the values of the ground-state variational parameters A and B that minimize the ground-state energy density. The energy is a very flat function near its minimum, and small irregularities due to statistical noise in the data make it difficult to determine values of B consistently. After trying several different approaches, the following procedure was adopted: Using Monte Carlo, the five measures given above were calculated at about 100 points that lie on a rectangular grid in A,B space. For each value of the coupling, the energy was calculated at all of the points. The coefficients of the paraboloid

$$E(A,B)=C_{00}+C_{10}A+C_{01}B+C_{11}Ab+C_{20}A^2+C_{02}B^2 \quad (18)$$

were determined by a local least-squares fit to the energies. The paraboloid then provided interpolation so that values of the energy at general A and B were available. This procedure also resulted in some smoothing of the Monte Carlo noise. The minimum energy and the corresponding values of A and B were then derived from the paraboloid. They are given in Table II at selected values of the coupling, and the energy is compared to the old variational energy as well as the exact energy in Fig. 2. The fit was made local by weighting each data point with a product of Fermi functions that cuts off the contribution from data distant from the point of interest, A_0. By iteration, the point of interest was kept very close to the point where the actual minimum was located, ensuring that the least-squares fit was localized appropriately. The Fermi function used is

$$W_i(A_i,A_0)=\left[1+\exp\left[\frac{|A_i-A_0|-2s}{s/4}\right]\right]^{-1}, \quad (19)$$

where s is the spacing in A between data points. This weight was multiplied by a similar function of the dis-

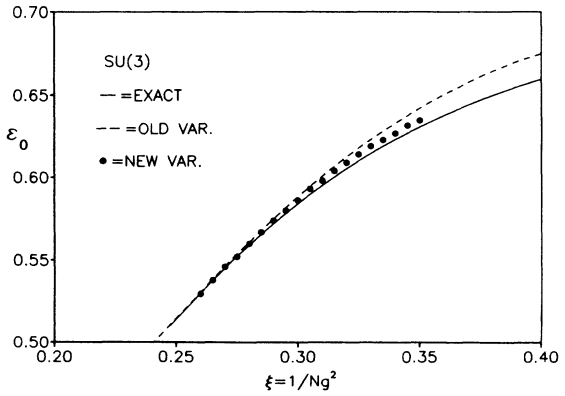

FIG. 2. The ground-state energy density for the gauge field sector of the Hamiltonian lattice QCD as a function of the coupling constant showing the improvement of the wave functions that include twisted loops (solid circles) over the one-parameter values (dashed line). The exact values obtained by the method of guided random walks are shown for comparison.

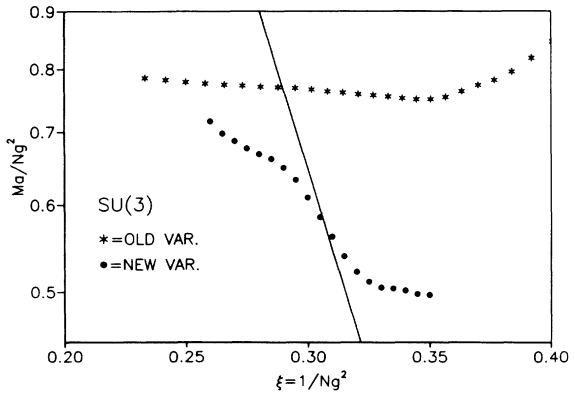

FIG. 3. The scalar-glueball mass estimate as a function of the coupling constant calculated using the one-parameter wave function (stars) compared to calculations using the improved wave functions (solid circles). The straight line gives the slope of the expected asymptotic scaling.

tance in the B direction to give a rectangular area of the A,B plane where data were included in the least-squares fit.

Having thus determined the A and B that minimize the energy for a given coupling, we used local paraboloid fits to each of the measures in order to determine their values and partial derivatives that were needed to minimize the scalar-glueball mass.

The results of the scalar-glueball mass calculations are shown in Fig. 3, and numerical values are given in Table II. Including the twisted loops in both the ground and excited states lowers the minimum of the glueball mass estimate ($Ma\xi$) from 0.76 to 0.50. This is a significant improvement, and the slope of the plot approaches that of the asymptotic scaling curve. Closer approaches have been achieved using Lagrangian methods.[10,11] The lack of scaling is not surprising when the minimum is compared to the minimum of about 0.30 obtained in the Lagrangian formulation by including all loops up to length 6^{10}. It seems that more types of loops will have to be included before true scaling appears.

IV. CONCLUSIONS

We have shown that including the twisted loops in the ground state and first excited state has a large effect on both the variational ground-state energy density and the scalar-glueball mass. Our wave functions for the scalar glueball are accurate enough in the intermediate coupling regime to show an approach toward scaling in SU(3). Since it appears that variational wave functions can be systematically improved by including additional loops, we plan to study the effects of other loops on the scaling behavior of the glueball mass.

ACKNOWLEDGMENTS

The calculations reported here were performed in part using the CYBER 205 at the Florida State University Supercomputer Research Institute. The work of C.L. and D.R. was supported in part by DOE Grant No. FG05-86-ER-40273. The work of S.A.C. was supported in part by NSF Grant No. PHY 86-08149.

[1]N. Kimura, Nucl. Phys. **B246**, 143 (1984); C. P. van den Doel and D. Horn, Phys. Rev. D **35**, 2824 (1987).

[2]S. A. Chin, O. S. van Roosmalen, E. A. Umland, and S. E. Koonin, Phys. Rev. D **3**, 3201 (1985).

[3]J. Kogut and L. Susskind, Phys. Rev. D **11**, 395 (1975).

[4]G. G. Batrouni, Nucl. Phys. **B208**, 467 (1982); H. Arisue, M. Kato, and T. Fujiwara, Prog. Theor. Phys. **70**, 229 (1983); Anthony Duncan and Ralph Roskies, Phys. Rev. D **31**, 364 (1985).

[5]S. A. Chin, Chris Long, and D. Robson, Phys. Rev. Lett. **57**, 2779 (1986).

[6]J. P. Greensite, Nucl. Phys. **B166**, 113 (1980).

[7]D. Robson, in Proceedings of the Workshop on Hamiltonian Lattice Gauge Theory and Monte Carlo Methods, Tallahassee, 1987 (unpublished).

[8]E. Dagotto and A. Moreo, Phys. Rev. D **29**, 2350 (1984).

[9]S. A. Chin, Chris Long, and D. Robson, preceding paper, Phys. Rev. D **37**, 3001 (1988).

[10]B. Berg and A. Billoire, Nucl. Phys. **B221**, 109 (1983).

[11]Ph. de Fourcrand, G. Schierholz, H. Schneider, and M. Teper, Phys. Lett. **152B**, 107 (1985); T. A. DeGrand, Phys. Rev. D **36**, 176 (1987).